Thermal structure of hot events and their possible role in maintaining the warm isothermal layer in the Western Pacific warm pool

Anindya Wirasatriya, Hiroshi Kawamura, Muhammad Helmi, Denny Nugroho Sugianto, Teruhisa Shimada, Kohtaro Hosoda, Gentur Handoyo, et al.

Springer

Thermal structure of hot events and their possible role in maintaining the warm isothermal layer in the Western Pacific warm pool

Anindya Wirasatriya[1,2] · Hiroshi Kawamura[3] · Muhammad Helmi[1,2] · Denny Nugroho Sugianto[1,2] · Teruhisa Shimada[4] · Kohtaro Hosoda[5] · Gentur Handoyo[1] · Yoppik Disma Girindra Putra[1] · Magaly Koch[6]

Abstract

The short-lived events of high SST are called hot events (HEs) and can only be generated under the conditions of large daily heat gain due to strong solar radiation and weak wind. We investigated the thermal structure below HEs in the western equatorial Pacific by using in situ data obtained from TAO/TRITON buoys. We found that the occurrence of HEs can be identified by the typical vertical thermal structure within the isothermal layer. During the development stage of a HE, heat is accumulated in the surface layer due to strong solar radiation and weak wind, increasing temperature and creating strong stratification in the upper layer. During the decay stage, strong westerly winds induce current convergence which transports the heat from the upper layer to the deeper layer. Thus, temperature decreases at the surface and increases in the deeper layer. Furthermore, this mechanism indicates the important role of HEs in maintaining the warm isothermal layer in the western Pacific warm pool. The more HEs occur, the more heat in the surface layer gained from solar radiation is transported to the deeper layer. This process makes areas of frequent HE occurrences coincident with areas of warm pool. Since surface winds control the heat accumulation and heat transport in the isothermal layer by influencing current divergence and latent heat flux, surface winds become the key factor for the occurrence of HEs and the formation of the thermal structure in the Pacific warm pool.

Keywords Short-term high · Thermal stratification · TAO/TRITON buoys · Western Pacific warm pool

1 Introduction

Sea surface temperature (SST) is a fundamental factor which is linked to the heat exchange at the interface of atmosphere

✉ Anindya Wirasatriya
aninosi@yahoo.co.id

1 Department of Marine Sciences, Faculty of Fisheries and Marine Sciences, Diponegoro University, Semarang, Indonesia

2 Center for Coastal Rehabilitation and Disaster Mitigation Studies, Diponegoro University, Semarang, Indonesia

3 Center for Atmospheric and Oceanic Studies, Graduate School of Science, Tohoku University, Sendai, Japan

4 Faculty of Science and Technology, Hirosaki University, Hirosaki, Japan

5 WNI Forecast Center, Weathernews Inc., Chiba, Japan

6 Center for Remote Sensing, Boston University, Boston, USA

and ocean. In the equatorial region, the temporal frequency distribution of the SSTs in a given region is characterized by a negatively skewed distribution (Clement et al. 2005; Waliser and Graham 1993). SSTs rarely reach 30 °C since such high temperatures require particular atmospheric conditions to occur, i.e., high solar radiation and low wind speed (Waliser and Graham 1993; Waliser 1996; Qin et al. 2007). Thus, for observing such high SST occurrences, high spatial and temporal resolutions of SST dataset are necessary. Otherwise, the existence of high SST may be concealed due to the interpolation process inherent at coarser resolutions.

By taking advantage of daily SST products with a spatial resolutions of 25 km derived from satellite observations, several studies (Kawamura et al. 2008; Qin et al. 2007, 2008; Qin and Kawamura 2009a, b, 2010; Wirasatriya et al. 2015, 2016, 2017) were able to identify high SST events in specific areas and at certain time periods and define them as hot event (HE). These studies focused on the atmospheric structure and SST in HE regions and their general conclusion was that the generation of a HE is characterized by significant daily heat gains of the surface water under the condition of high solar radiation

and low wind speed. This condition is formed as the result of "remote convection" mechanism, a convection that occurs at remote area and causes air subsidence on the HE area.

On the other hand, the oceanic structure during the HEs has received less attention by previous HE studies. Qin and Kawamura et al. (2008) and Wirasatriya et al. (2015) found a strong thermal stratification of a water column during the HE occurrence and associated large diurnal amplitude of SST. However, their analyzes were based only on a limited number of Triangle Tropical Atmosphere Ocean/Trans-Ocean Buoy Network (TAO/TRITON) buoys, and thus, the horizontal distribution of the thermal structure has not been considered yet. In this study, a larger number of TAO/TRITON buoys are used to explore the oceanic thermal structure of the various HEs that were not considered in the previous studies.

Western Pacific warm pool is a region with the most frequent HE occurrence (Qin et al. 2007; Wirasatriya et al. 2015). On the other hand, the warm mixed layer in the western Pacific warm pool plays an important role in the coupled ocean-atmosphere dynamics and thermodynamics which influences the variability of the global climate (e.g., Clement and Seager 1999; Herweijer et al. 2005). Thus, it is important to understand the formation process of the warm pool. Clement et al. (2005) used an atmosphere-ocean coupled model to investigate the formation of the western Pacific warm pool. They explained that under easterly wind stress, the thermocline is deep in the west and shallow in the east. The easterly wind stress induces poleward Ekman transport of water in the surface layer. The water is compensated by equatorward geostrophic flow below and by equatorial upwelling, which creates a cold tongue in the east but homogenizes SST in the west or a warm pool. Their analysis, however, was based on an annual mean dataset which cannot detect the highly intermittent wind events in the western equatorial Pacific. Thus, the present study investigate the mechanisms of how surface wind forcing controls the heat transport in the isothermal layer of the western Pacific warm pool at shorter time intervals than in the previous studies following the criteria established for defining a HE.

The relationship between the western Pacific warm pool and HE was investigated and statistically explained by Wirasatriya et al. (2015) who compared the long-term mean SST, as a measure of the warm pool, to the HE occurrence rate (Fig. 1). The study showed that an increase in the frequency of HE occurrences results in higher climatological mean SST in the western equatorial Pacific. In the warm pool area enclosed by the 29.5 °C isotherm of the climatological SST, HEs coincide with SST greater than 30 °C with a percentage of 51.5%. However, the physical processes underlying the relationship between HEs and warm pools were not clarified in their analysis.

The temperature variability of the mixed layer in the warm pool is influenced by the heat flux, momentum flux, and mass flux. By using single buoy analysis centered in the warm pool and 1D model, Anderson et al. (1996) found that the mass exchange between the ocean and atmosphere such as water vapor and rainfall are as important as the heat exchange to maintain the temperature of mixed layer of the western Pacific warm pool. In the present study, we focused on the analysis of the heat flux and momentum flux associated with the surface wind forcing to understand the mechanism of a HE which forms only under clear sky and calm conditions. We used observations of TAO/TRITON buoys deployed evenly in the western equatorial Pacific to investigate the thermal structure of HEs as well as the possible role of HEs on regulating the warm isothermal layer in the western Pacific warm pool.

2 Data and methods

We use the New Generation Sea Surface Temperature for Open Ocean (NGSST-O-Global-V2.0a) to identify HEs in the western equatorial Pacific (Hosoda 2013) during 2003–2011. This dataset is the result of merging SST observations acquired by two satellite microwave sensors (AMSR-E onboard Aqua and WindSat onboard Coriolis) after applying diurnal corrections to estimate 1 m depth SST at the local time of dawn (06:00LT) and at each longitude. The interpolation method follows Hosoda et al. (2015) approach, and uses daily data at grid intervals of 0.25° × 0.25°. The bias and root mean square error against the TAO/TRITON buoy SST in the study area is −0.107 °C and 0.428 °C, respectively.

Following the definition of HE in Wirasatriya et al. (2015), the HE is defined as a connected region with a SST higher than the space-time dependent threshold (around 30 °C), with an areal size larger than 2×10^6 km, and lasting for a period longer than 6 days. The space-time dependent threshold is produced by first, calculating the background SST by averaging the daily variation of SST at all grids in the area inside the 27 °C isotherm in the western equatorial Pacific. Next, the daily mean SST was low-pass filtered with a 101-day cutoff. Finally, the threshold is defined as the filtered background SST plus 1.4 °C so that the mean of the HE threshold is 30 °C. The details of the HE detection method and their explanation are described in Wirasatriya et al. (2015). Following Wirasatriya et al. (2016), the present analysis also considers the development stage and decay stage of HE. The development stage is defined as the period of time from the day when the areal size starts to increase to the day when
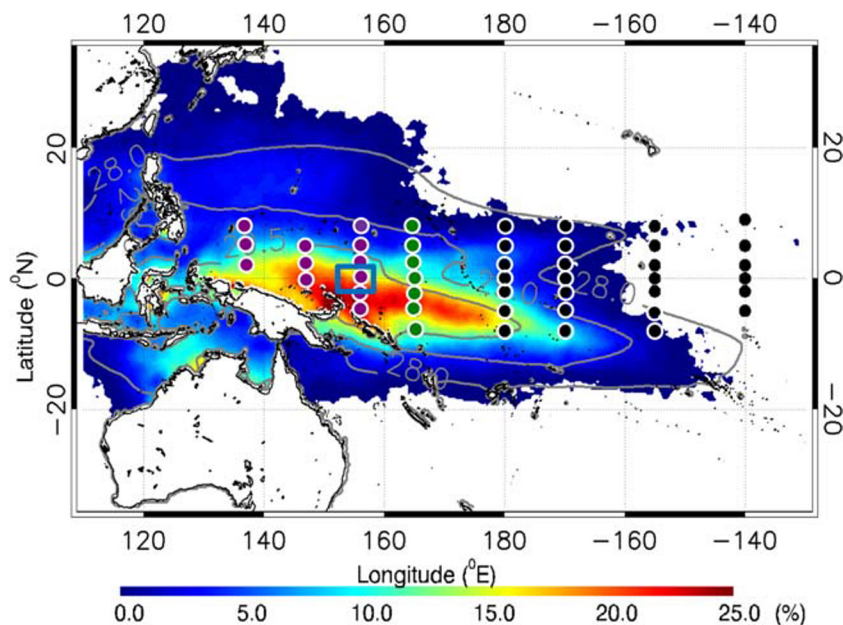
Fig. 1 Occurrence rates of HEs shown in frequency per bin (%) during 2003–2011 (100% is 3163 days; » 9-year period). The gray contour represents the mean SST climatology for the period of 2003–2011) from NGSST-O-Global-V2.0a data (Hosoda 2013; Hosoda et al. 2015). The dots are the positions of TAO/TRITON buoys used in the analysis. All dots are the positions of the buoys for SST, subsurface temperature and surface wind measurements used in the analysis. The purple and green dots are the TAO/TRITON buoys for solar radiation measurements. The purple dots are the position of subsurface density (st) measurements used in the analysis (modified from Wirasatriya et al. 2015). Blue box denotes the chosen area for time series analysis shown in Fig. 3, 5, 7, 9 and 10

the areal size reaches its maximum. The decay stage is defined as the period of time from the day when the areal size begins to decrease from its maximum to the day when the areal size reaches its minimum. The detailed definition of development and decay stage can be found in Wirasatriya et al. (2016).

We use daily measurements data from the TAO/TRITON buoys (McPhaden et al. 2009) located at the western equatorial Pacific (Fig. 1). The parameters used in this study are temperature (surface and subsurface), surface wind, solar radiation, and subsurface density (ρ_τ). Since the data consist of six quality grades, only the data with the highest and the default quality are used in the analysis. The data with the highest quality satisfy pre/post-deployment calibrations and the data with the default quality satisfy either pre-deployment calibrations only or post-deployment calibrations. The position and depth interval of TAO/TRITON buoys for the measurements of temperature, and density are shown in Fig. 2. Subsurface temperature and density are linearly interpolated into 1 m, 10 m, 20 m, 30 m, 40 m, 50 m, 60 m, 70 m, 80 m, 90 m, and 100 m. We calculated ocean heat content for each layer from subsurface temperature and density following the equation:

$$H = \rho_\tau \, C_p \int_{h2}^{h1} T(z)dz \qquad (1)$$

where H is heat content (J/m^2), ρ_τ is sea water density (kg/m^3), C$_p$ is heat capacity of the ocean $\approx$ 4184 J/KgK, T is temperature (K), z is depth (m), h$_2$ and h$_1$ are the deeper and shallower depths, respectively. We use a critical temperature gradient of 0.02 °C/m to determine isothermal layer depth following the criteria of Wyrtki (1964) and Bathen (1972). Then, all parameters are interpolated into 1°grid intervals by the quintic method, i.e. grid points are interpolated with quintic polynomials from triangles formed by Delaunay triangulation (Akima 1996; Renka 1984).

We also use daily surface current from GLOBAL-REANALYSIS-PHY-001-025, a Mercator reanalysis dataset with grid interval 0.25° (Garric and Parent 2018a). This data is in well accordance with the equatorial moorings observations (Garric and Parent 2018b). Then, surface current divergence is calculated from the surface current data. The solar radiation, longwave radiation, surface wind speed, sensible heat flux, latent heat flux and net heat flux are obtained from Objectively Analyzed Air-Sea Fluxes project (OAFLUX) (Yu and Weller 2007). For precipitation, we used 3 h real time Tropical Precipitation Measuring Mission (TRMM) Multi-satellite precipitation analysis (3B42 RT) (Huffman et al. 2014).

Following Wirasatriya et al. (2015), HE is named as HEyymmdd, where "yy", "mm", and "dd" are respectively year, month, and day when the HE started. We conduct a case study for a HE that occurred on 28 May 2003 (called HE030528) to obtain the characteristics of its oceanic structure. This analysis will complete the understanding of
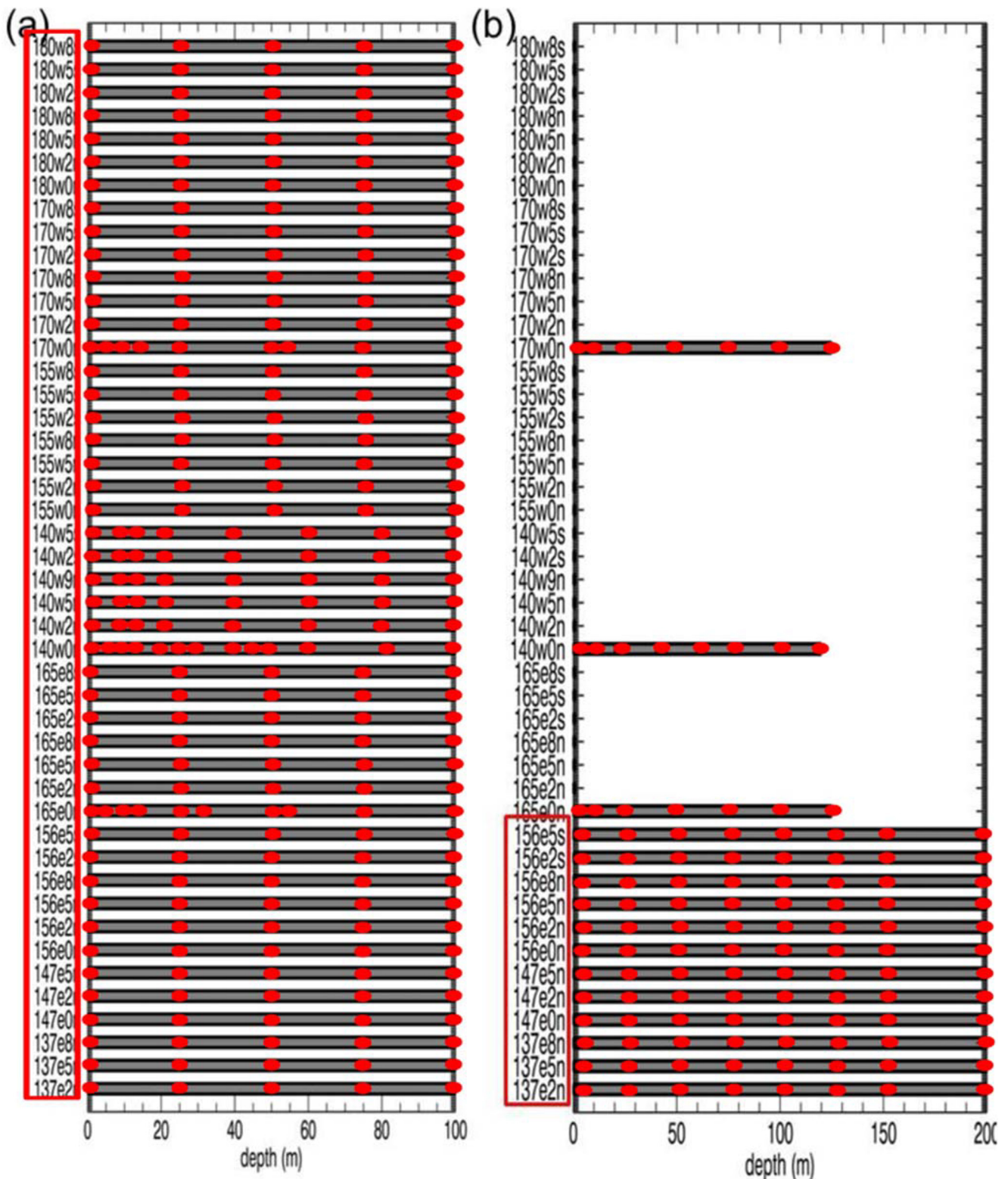
Fig. 2 Data availability of TAO/TRITON buoy for the measurement of **a** temperature, and **b** density in the study area. The depths of measurement are denoted by the red dots. The *red boxes* denote the chosen buoy for density measurements

HE mechanism since its atmospheric structure was studied by Wirasatriya et al. (2016). Afterwards, we compare the oceanic thermal structure between the periods with the frequent HE occurrence and without HE occurrence to investigate the role of HEs for the formation of the western Pacific warm pool.
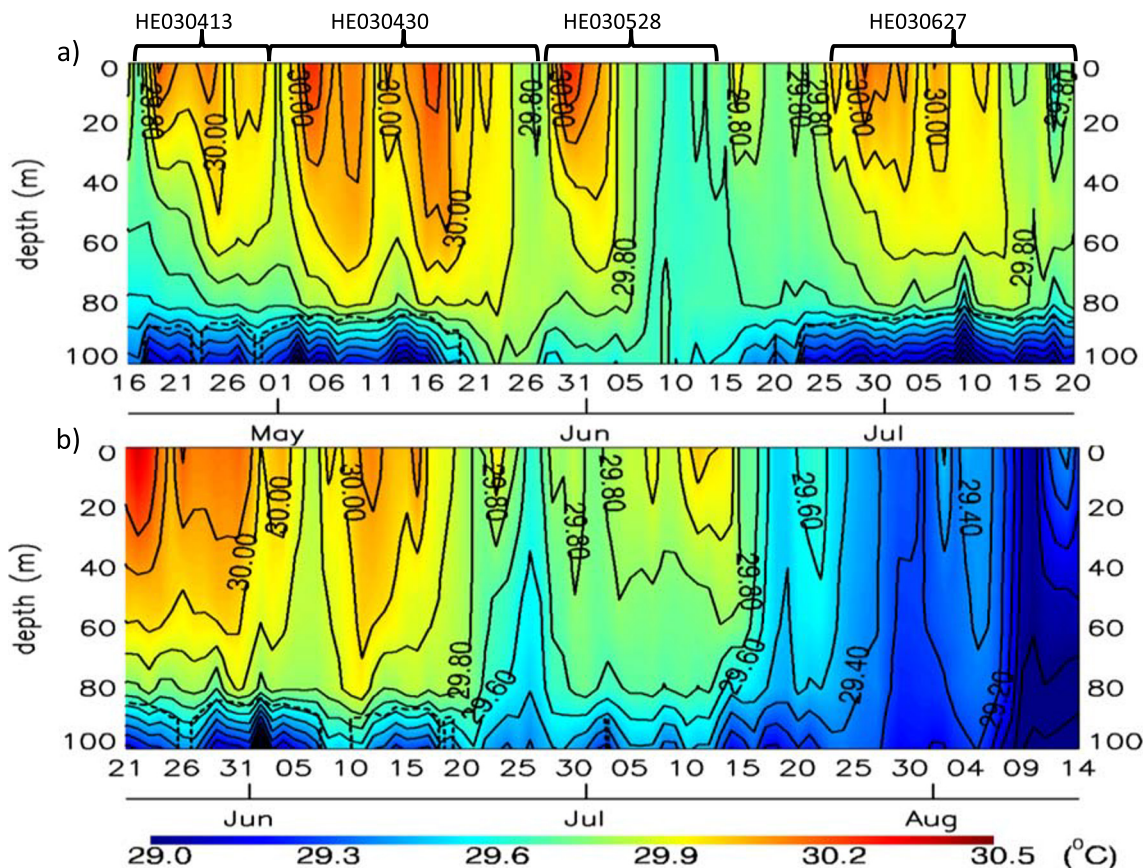
Fig. 3 The time series of subsurface temperature in **a** 2003 and **b** 2010 at 152°E-157°E and 3°S-3°N (*Blue box* in Fig. 1). *Broken contour* denotes isothermal layer depth or thermocline depth (vertical gradient temperature = 0.02 °C/m), *solid contour* denotes subsurface temperature

3 Result

3.1 Thermal structure characteristics of HEs

To obtain the thermal structure characteristics of a HE, we compared the thermal structure of the western Pacific warm pool during the period with frequent HE occurrence in 2003 (Fig. 3a) and without HE occurrence in 2010 (Fig. 3b). The area of 152°E-157°E, 3°S-3°N was chosen for the analysis since this area is located at the frequent HE area as shown in Fig. 1 and the buoys located in this area measured all parameters described in the previous section (c.f. Fig. 2).

A period of high HE activity was observed in 2003 and was represented by the occurrence of four HEs within 3 month period of observations as collected by Wirasatriya et al. (2015) i.e. HE030413 in mid-April 2003, HE030430 in mid-May 2003, HE030528 in late May 2003, and HE030627 in late Jun 2003 (Fig. 3a). The depth of thermocline layer is about 80 m. During this period, the temperature in the isothermal layer is warm ranging from 29.8 °C to 30.3 °C. It is also observed that the temperature of the isothermal layer reaches a peak within each HE period. In contrast, we can see the temperature decrease in the isothermal layer during the period without HE occurrence in 2010 (Fig. 3b). At the end of May 2010, the temperature of isothermal

layer is about 30 °C and at the beginning of August 2010 temperature drops into ~29.4 °C. The thermocline layer is deep during the period without a HE event, reaching more than 100 m depth which exceeds the depth of observations. The stratification during the period with frequent HE occurrence is more intensified and the temperature is warmer than during the period without HE occurrence. The stratified temperature structure is denoted by the narrower temperature contours during the period of HE occurrence. This result indicates that, in terms of vertical thermal structure, HE is characterized by the warm and stratified water column. To focus on the detailed thermal structure of a HE, we show a case study in subsection 3.2. Furthermore, the possible mechanisms underlying the relation between HE occurrence and warm pool formation are also investigated through a case study in subsection 3.3.

3.2 Mechanism of stratified thermal formation during HE period

To investigate the detailed thermal structure during a HE period, a case study of HE030528 was conducted. The atmospheric structure of HE030528 has been explained by Wirasatriya et al. (2016) who shows the significant difference of atmospheric structure between the development and decay stage of HE. During the
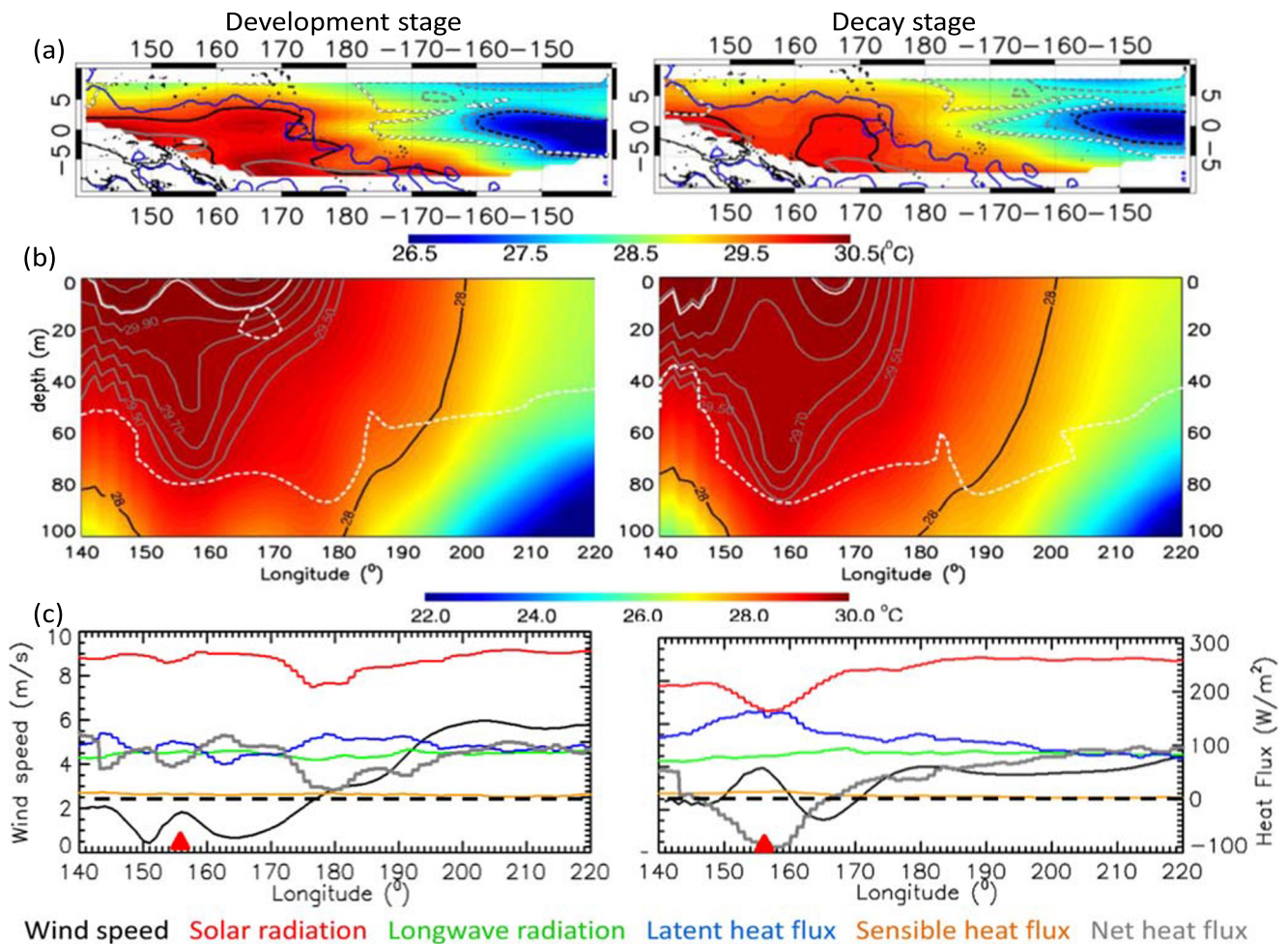
Fig. 4 **a** Sub-surface temperature composites of the development and decay stage of HE030528. *Blue line* is the area of HE030528 occurrence obtained by NGSST. *Black, gray,* and *white solid lines* denote temperature of SST threshold at 1 m, 40 m and 80 m depth, respectively. *Black, gray,* and *white broken lines* denote 27 °C at 1 m, 40 m and 80 m depth, respectively. Both solid and broken lines obtained by the buoy observations. **b** Zonal section of subsurface temperature composites (3°S-3°N) of the development and decay stages of HE030528. The *solid (broken) white*

contour denotes the SST threshold (isothermal layer depth ≈ vertical gradient of 0.02 °C/m). **c** Wind speed composite and heat flux composites from OAFLUX, i.e., solar radiation (positive downward), longwave radiation (positive upward), latent heat flux (positive upward), sensible heat flux (positive upward), and net heat flux (positive downward) (3°S-3°N) of the development and decay stages of HE030528. *Red triangle* in the longitude indicates the robust influence of surface wind speed and solar radiation on the thermal structure of HE (see text for more explanation)

development stage, surface wind speed is low, reducing the latent heat release. On the other hand, the subsidence of the air mass from the top of troposphere gives positive feedback to suppress the convection and eventually increase solar radiation. During the decay stage, surface wind speed is high and strong convection occurs, which accelerates the cloud formation that reduces solar radiation. Following Wirasatriya et al. (2016), thermal structure of HE030528 was also investigated by separating the analyzes in development and decay stages.

The first step of the investigation is the composite analysis of parameters during the development and decay stage of HE030528 (Fig. 4). During the development stage of HE, thermal structure is obviously different from the decay stage. Figure 4a and b show that the temperature is higher during the development stage than during the decay stage. Figure 4a shows that during the development stage the area enclosed by isotherm of SST threshold at 1 m

depth of TRITON buoy (*solid black line*) almost coincides with the area of HE030528 represented by the contour of NGSST threshold (*solid blue line*). Moreover, this also implies that the spatial pattern of interpolated TRITON SST is consistent with that of NGSST. During the decay stage, the contour of the SST threshold at 1 m depth shrinks indicating a decrease of SST. The vertical section shown in Fig. 4b also shows the consistent variation. Moreover, different thermal stratifications between the stages are identified in Fig. 4b. Figure 4b shows that the temperature contours during the development stage are narrower to each other than during the decay stage. This indicates that vertical temperature is more stratified during the development stage than during the decay stage. Thus, the composite analysis shows that the development stage of HE is characterized by a warmer and more stratified surface layer (< 20 m) than during the decay stage. Moreover, Fig. 4a also shows that at the eastern side where there
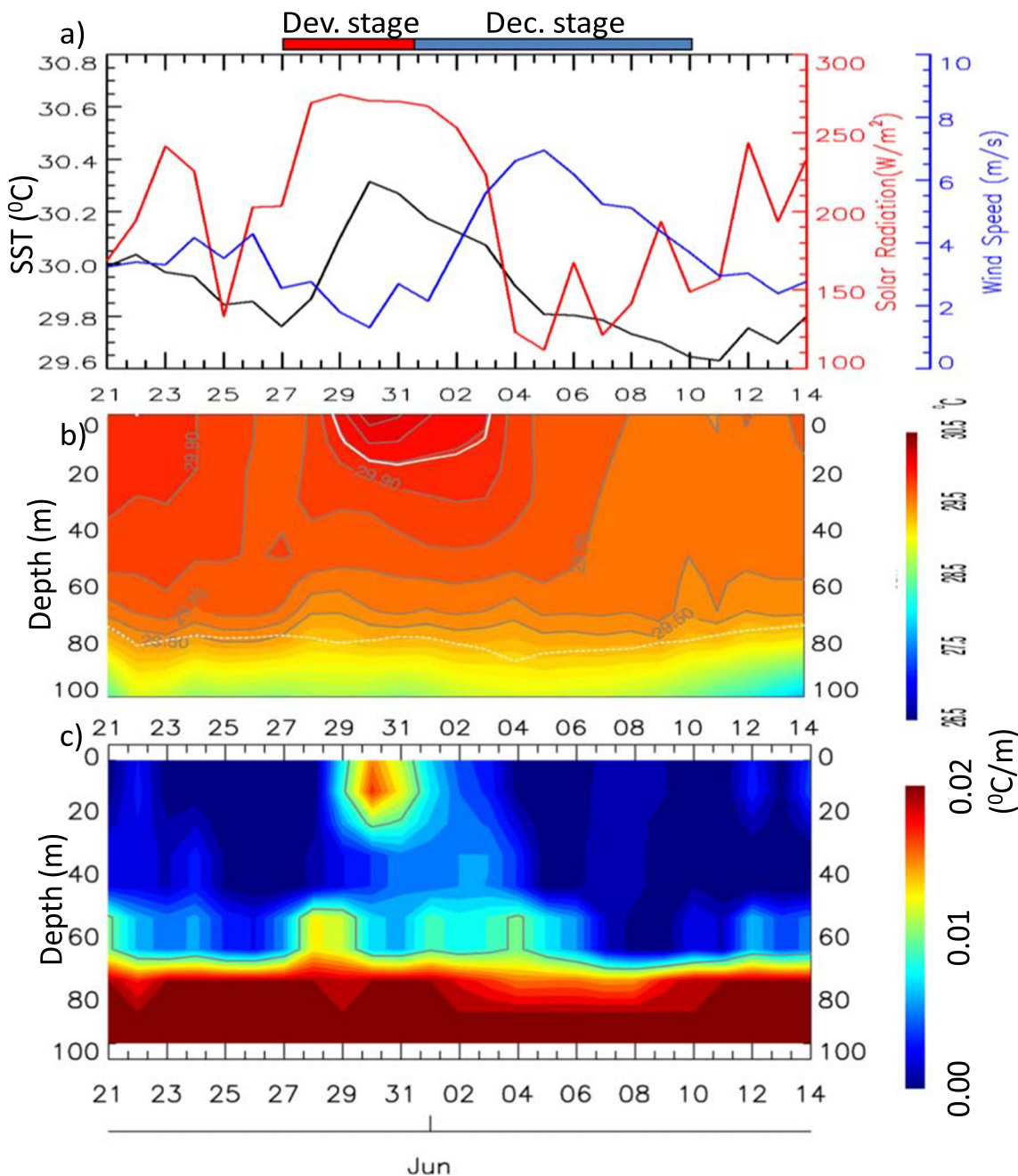
Fig. 5 The time series of oceanic and atmospheric features for HE030528 at 152°E-157°E and 3°S-3°N (*Blue box* in Fig. 1). **a** Surface temperature, wind speed, and solar radiation. **b** Subsurface temperature. *Solid (broken) white contour* is the SST threshold (isothermal layer depth). **c** Vertical temperature gradient. *Gray line* denotes the gradient temperature 0.01 °C/m

is no HE, the temperature is lower and less stratified than at the western side for both composited stages denoted by the coinciding contours of 27 °C at 1 m and 40 m depth.

The thermal stratification during the development and decay stages of HE shows a significant relationship with heat flux (Fig. 4c). For the heat flux component driven by wind speed, latent heat flux has a much larger magnitude (more than 100 W/m^2), than sensible heat flux (only less than 5 W/m^2). This means that disequilibrium in humidity plays a more substantial role than the disequilibrium in temperature between air and sea surface in

determining the heat flux in the western equatorial Pacific. Similar indication is also found in the Java Sea as observed by Wirasatriya et al. (2019). Furthermore, there is almost no difference for the distribution of longwave radiation and sensible heat flux between development and decay stage of HE. Surface wind speed during the development stage is lower (about 2 m/s) than during the decay stage (about 4 m/s) at the HE area (140°E-170°E). The variation of wind speed corresponds to that of latent heat release which shows lower latent heat release during the development stage (about 100 W/m^2) and higher during the decay
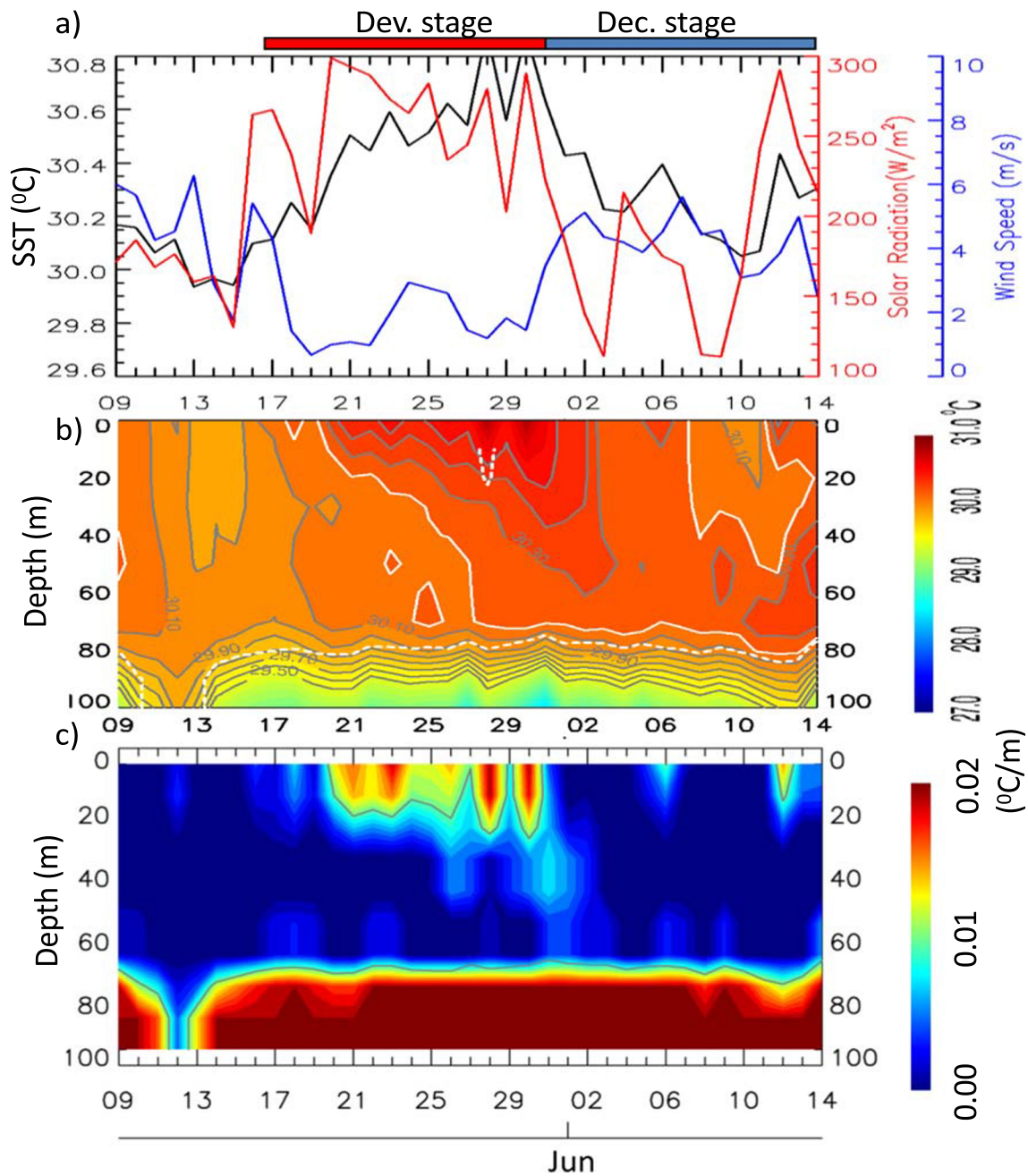
Fig. 6 As in Fig. 5, but for for HE041216 at 165°E-170°E, 5°S to 0°N

stage (about 150 W/m^2). In contrast, solar radiation is higher during the development stage (about 250 W/m^2) than during the decay stage (less than 200 W/m^2). This means that wind speed and solar radiation are the main heat flux components that influence the occurrence of HEs. This result supports Wirasatriya et al. (2015). Results of all heat flux aspects are represented by the net heat flux which shows the net heat gain (i.e., positive net heat flux) during the development stage and net heat release (i.e., negative net heat flux) during the decay stage. This result is consistent with Qin and Kawamura (2009b) who found the positive heat gain during HE formation. Furthermore, the influence of surface wind speed and solar radiation on the thermal structure is

observed more clearly at around 155°E (red triangle in Fig. 4c). The contour of temperature threshold extends to the surface due to the higher surface wind speed and lower solar radiation than its surroundings.

The second investigation is the time series analysis shown in Fig. 5. The variation of wind speed and solar radiation corresponds to the variation of SST and subsurface temperature (Figs. 5a and b). During the development stage, wind speed decreases from 4 m/s to 1 m/s and solar radiation increases from 140 W/m^2 to 250 W/m^2. This causes SST to increase from 29.8 °C to 30.2 °C. The temperature of the subsurface layer from
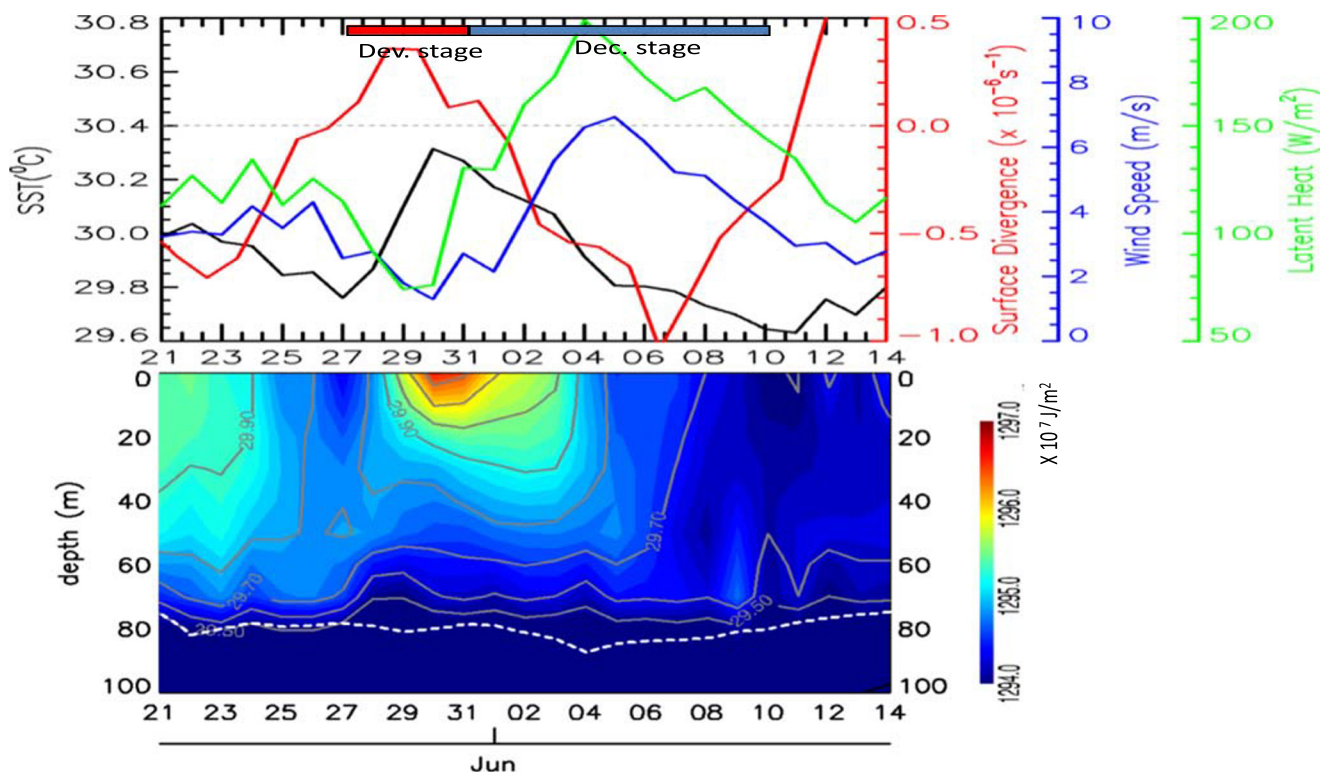
Fig. 7 The time series of temperature at 1 m depth, wind speed, surface current divergence, latent heat (upper panel), and heat content (lower panel) for HE030528 at 152°E-157°E and 3°S-3°N (*Blue box* in Fig. 1).

Broken white contour denotes isothermal layer depth (vertical gradient temperature = 0.02 °C/m) and *solid gray contour* denotes subsurface temperature

0 m to ~ 50 m increases during the development stage. On 27 May 2003, subsurface temperature was vertically uniform at around 29.8 °C. Along with the increasing solar radiation and decreasing wind speed, increasing rate of subsurface temperature varies with depth. At the surface layer temperature reaches 30.2 °C on 31 May 2003, while at 20 m depth it reaches 29.9 °C. This indicates an intensified stratification during the development stage of HE. The evidence of intensified stratification is more clearly seen in Fig. 5c. A strong stratification with temperature gradient greater than 0.01 °C/m can be observed during 29–31 May 2003, from the surface to 30 m depth. Below 30 m, the temperature is lower (< 29.8 °C) and more uniform than above 30 m. During the decay stage, the wind speed increases from 1 m/s to 6 m/s and solar radiation decreases from 250 W/m² to 100 W/m² causing the decrease and uniformity of temperature. Above 30 m depth, temperature decreases to 29.8 °C on 4 Jun 2003. From 30 m to 50 m depth, temperature increases beyond 29.8 °C on 4 Jun 2003. After 4 Jun 2003, the temperature from surface to 60 m depth continues to decrease and becomes uniform. In the cases of HE with longer duration, higher solar radiation, and weaker wind speed, this indication becomes more pronounced. We used HE041216 which was also investigated by Wirasatriya et al. (2015) as a case study for the longer duration HE (Figs. 6a and b). The contour of temperature threshold of HE041216 can penetrate deeply approaching the thermocline (about 80 m depth) which might correspond to

higher solar radiation (about 300 W/m²) and lower surface wind speed (less than 2 m/s) during the development stage than the case HE030528. Thus, the vertical thermal structure of the development stage of HE is characterized by increasing temperature and an intensified stratification at the surface layer due to the surface heating. During the decay stage, surface layer temperature becomes lower and the deeper layer becomes warmer. As a result, vertical thermal structure becomes uniform during the decay stage.

Combining these findings with the result from Wirasatriya et al. (2015) which provide the time series analysis of hourly buoy data of temperature at the sea surface, 25 m depth and 50 m depth for HE041216 (Fig. 3b of Wirasatriya et al. (2015)), it can be seen that the surface layer stratification during the development stage of HE041216 corresponds to the high amplitude of diurnal SST. Moreover, this time series analysis also shows warmer and more intensively stratified waters during the development stage than during the decay stage. It also should be emphasized that during the development stage, only the temperature at the surface layer increases. After the increase of surface wind speed and the decrease of solar radiation during the decay stage, the temperature decreases at the surface layer but increases at the deeper layer. This process decreases the temperature difference between surface and deeper layers, resulting in a more uniform temperature distribution. Furthermore, wind speed and solar radiation seem to exert an influence on temperature and stratification variations
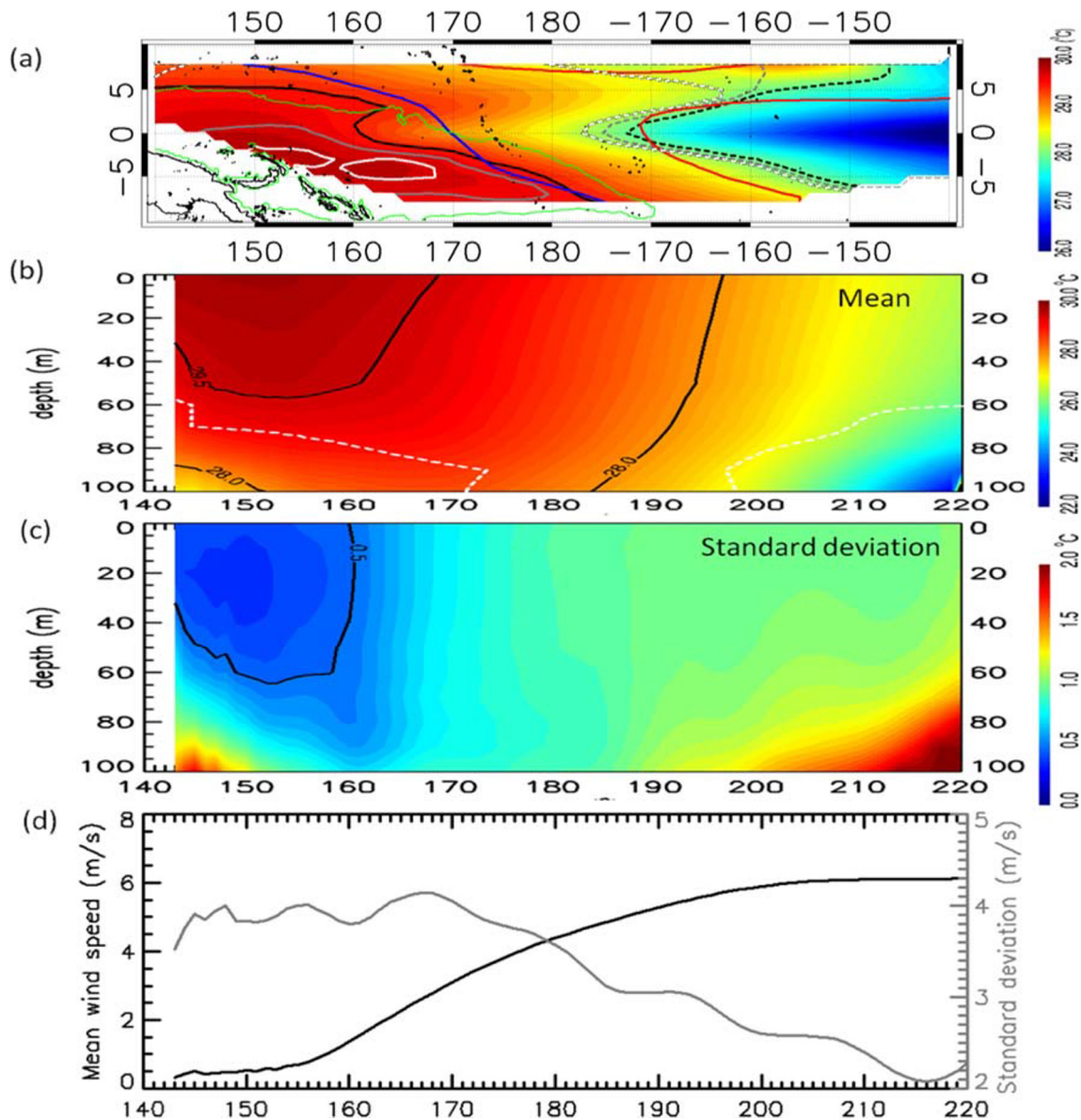
Fig. 8 a The SST (T1m) climatology map of western equatorial Pacific. *Black, gray,* and *white contours* denote SST, temperature at 40 m and temperature at 80 m, respectively. *Solid* and *broken contours* denote the isotherm of 29.5 °C and 28 °C. *Blue* and *red contours* denote 3.5 m/s and 5.5 m/s wind speed, respectively. *Green contour* represents the frequent HE area with the occurrence rate of more than 10%. **b** and **c** Zonal section (5°S-0°N) of climatological mean and standard deviation of sub surface temperature. *Broken white contour* is the isothermal layer depth ≈ vertical gradient of 0.02 °C/m. **d** Zonal section (5°S-0°N) of climatological mean and standard deviation of wind speed

only within the isothermal layer. This is supported by the fact in the present study that no influence of HE occurrences on temperature that could be detected below the thermocline layer around 80 m depth (Fig. 6b).

The mechanisms of the thermal structure of HE can be explained by variations in surface current and latent heat flux (Fig. 7). During the development stage, the water column in the isothermal layer is relatively stable denoted by the small current divergence. This means that there is almost no vertical movement of the water mass during the development stage. Latent heat release is also low. Thus, the heat received

from the solar radiation is kept and accumulated at the sea surface, causing the increase of SST and thermal stratification. This condition creates the first half of HE thermal structure, i.e., the development stage. During the decay stage, downwelling and horizontal mixing occur, denoted by the increase of current convergence. Lukas and Lindstorm (1991) reported that westerly winds straddling the equator cause an Ekman convergence at the equator, resulting in a downwelling response in that area. Moreover, latent heat release becomes high. Hence, the accumulated heat gained during the development stage is transported to the deeper layer through the downwelling process as the heat
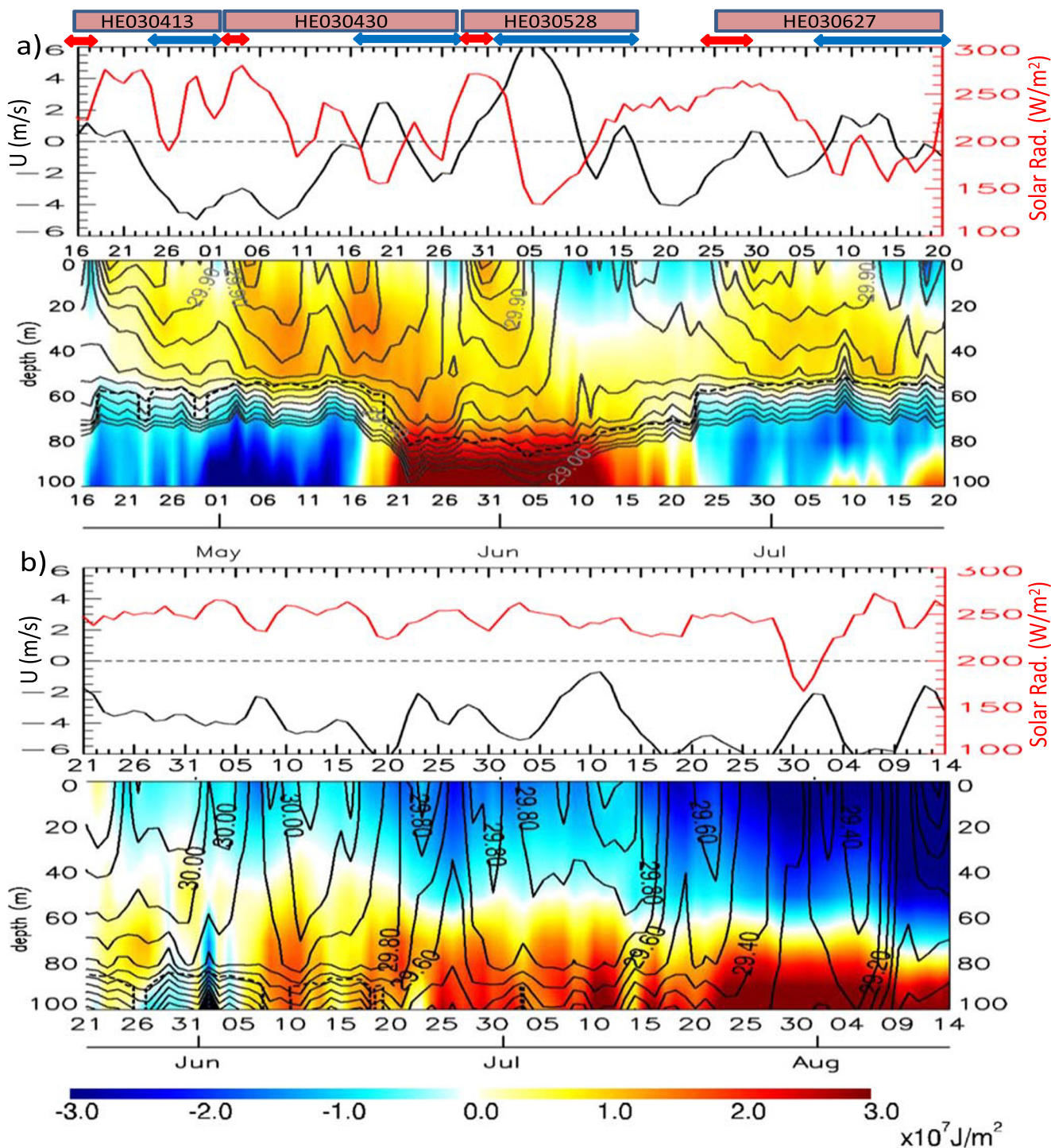
Fig. 9 The time series of zonal wind component, solar radiation, and heat content (shading) in **a** 2003 and **b** 2010 at 152°E-157°E and 3°S-3°N (*Blue box* in Fig. 1). The heat content was normalized by subtracting to the first date's value. *Broken contour* denotes isothermal layer depth (vertical gradient temperature = 0.02 °C/m), *solid contour* denotes subsurface temperature as shown in Fig. 3. Zonal wind and solar radiation were smoothed by 3 days average. The *red* and *blue double arrow* in upper figure denotes the development and decay stage of HE, respectively

is also released to the atmosphere through the increase of latent heat release during the decay stage. The consequence is lower temperature at the surface and higher temperature at the deeper layer which makes the vertical distribution of temperature becomes more uniform. This condition creates another half of the HE thermal structure, i.e., the decay stage. Therefore, the thermal structure of HE represents the heat mixing mechanism in the isothermal layer.

3.3 The physical process underlying the relationship between hot events and the Pacific warm pool

To explain the mechanism underlying the relation between HE and the Pacific warm pool, first we show the climatological analysis of the western Pacific warm pool in Fig. 8. The western equatorial Pacific is characterized by warmer and more stable stratified layers in the western side (140°-170°E) than in the central side (170°-200°E) (Figs. 8a–c). The stable isothermal layer is denoted by the small standard deviation of water temperature, i.e., less than 0.5 °C (Fig. 8c). The thermal structure is characterized by the stratification in the western side and uniform in the central side. The stratification at the western side is shown by the different positions of the 29.5 °C contour at the surface (SST), at 40 m, and at 80 m depth. In contrast, the position of the 28 °C contour at the surface, at 40 m and at 80 m depth coincides with each other in the central part of the equatorial Pacific. Thus, the isothermal layer depth at the western side is shallower than the central side (Fig. 8b). This thermal structure pattern is consistent with previous studies (e.g., Lukas and Lindstorm 1991; Ando and McPhaden 1997).

The relationship between HE and the western Pacific warm pool is also shown in Fig. 8a. The area with the frequent HE occurrence is located in the western side of the equatorial Pacific where SST is more than 29.5 °C and more stratified than the central side

(Figs. 8a and b). Furthermore, Fig. 8c also shows that the western side of the equatorial Pacific is more stable denoted by the standard deviation less than 0.5 °C. The warm and stable water mass may be favorable for HE generation.

To emphasize the importance of the mechanism of vertical thermal structure of HEs for the formation of the western Pacific warm pool, we modified Fig. 3 by overlying the contour of temperature and oceanic heat content (Fig. 9). The characteristic of vertical thermal structure during a HE is detected in mid-April 2003 which is HE030413. This indication continues in HE030430 (late April 2003 and mid-May 2003), HE030528 (late May 2003) and HE030627 (late Jun 2003). We can also see the accumulated heat at the surface during the development stages and sensible heat transfer from the surface to the deeper layer during the decay stages, which is the mechanism responsible for forming the vertical thermal structure of HEs. It is also noted that except for HE030413, their development and decay stages is controlled by the zonal wind variation as explained in Wirasatriya et al. (2016); weak wind during the development stage and strong westerly wind during the decay stage. In HE030413, the decay stage is denoted by the strong easterly wind. In 2010, the vertical thermal structure featuring HE is not detected, suggesting that sensible heat was not adequately transferred to the deeper layers. The easterly wind is consistently strong during all period.

Fig. 10 The time series of precipitation (upper panel) and density (lower panel) for HE030528 at 152°E-157°E and 3°S-3°N (*Blue box* in Fig. 1). *Solid gray contour* denotes the density contour at 21.2 kg/m³
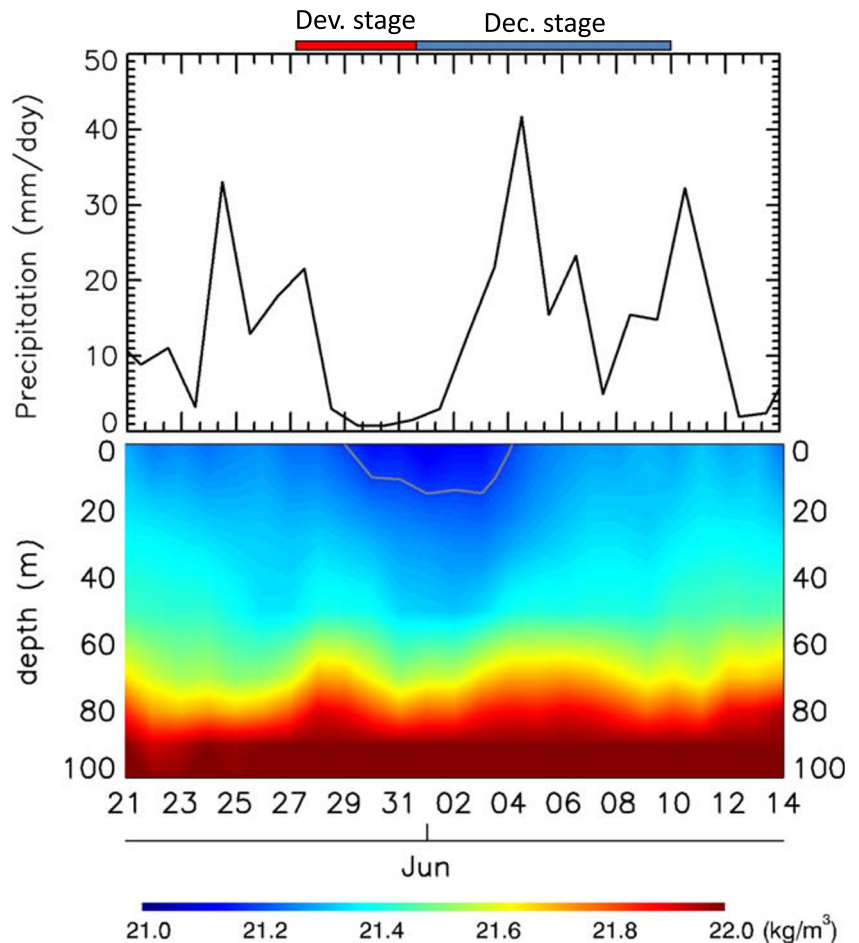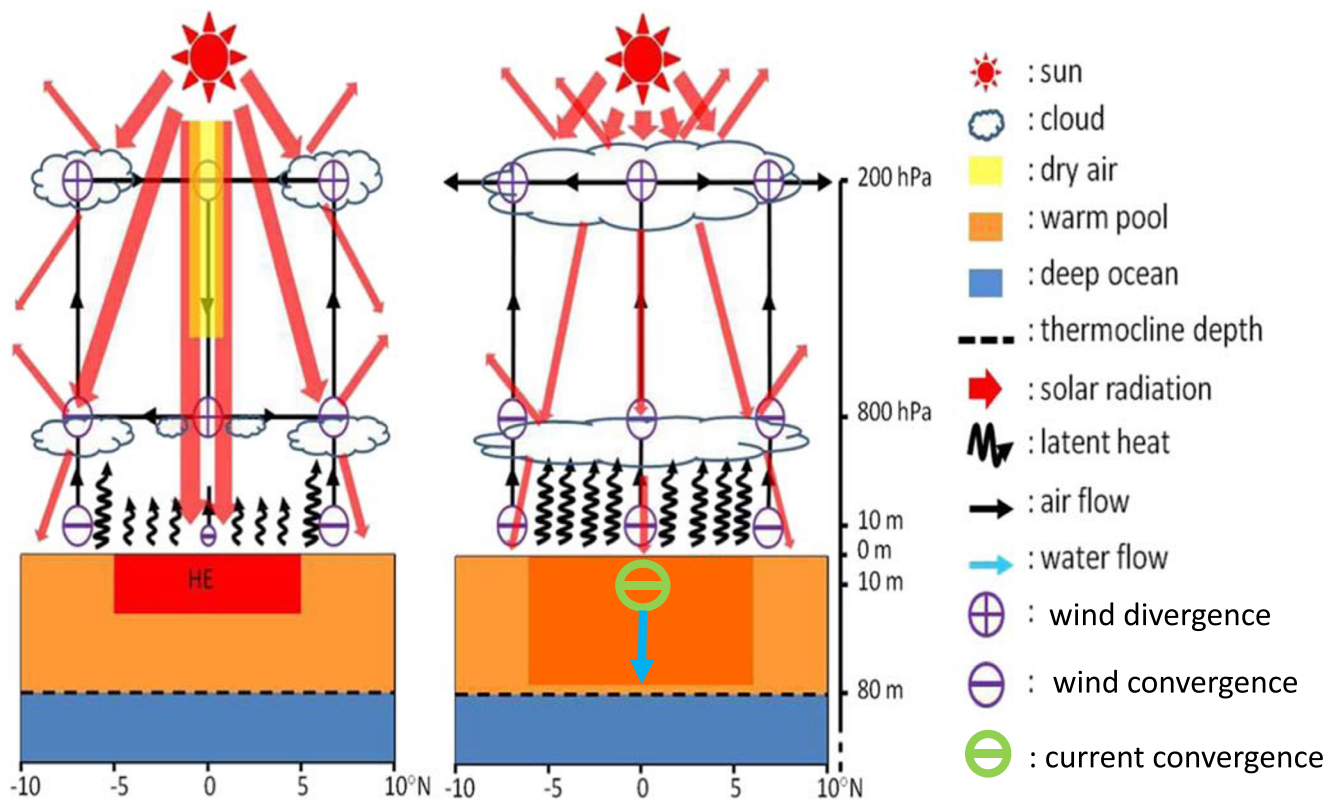
Fig. 11 Scenario of the HE030528 mechanisms in the western equatorial Pacific. Left and right figures denote the development and decay stage, respectively

As a result, the water temperature at the period of 2003 is warmer than the water temperature at 2010 (Fig. 3) since more sensible heat is transported to the deeper layer in 2003 (Fig. 9). The warm subsurface temperature is maintained during 2003. Conversely, at the end of the 2010 period, the subsurface temperature was cooler than at the beginning of this period. It can be concluded that HE plays an important role in maintaining the warm isothermal layer in the western Pacific warm pool by transporting the sensible heat accumulated at the surface during the development stage of HE to the deeper layer during the decay stage. Since a warm pool may provide favorable conditions for HE generation, this process becomes the positive feedback of HE to the Pacific warm pool formation. This result becomes the physical evidence of the relation between HEs and the Pacific warm pool that was first statistically revealed in Wirasatriya et al. (2015). Moreover, this result also emphasizes the role of surface wind as a key factor for the HE generation since the surface wind controls current speed, current divergence, and latent heat flux during the HE occurrence.

4 Discussion

In this section we discuss the other factors influencing the warm pool formation. We also compare the thermal structure of HE discussed by Qin et al. (2008) and the present study. Furthermore, we combined the present result with the result of

the previous studies to link the oceanic factors to the atmospheric factors involved in the HE generation to enhance our understanding of possible mechanisms of HE formation.

In general, the formation mechanisms of vertical thermal structure in the near surface ocean have been widely known as shown systematically by Marshall and Plumb (2008), and involve momentum flux, mass flux, and radiation flux. Momentum flux is driven by the surface wind while mass flux is driven by the buoyancy forcing induced by precipitation and evaporation. Lukas (1988) stated that the importance of wind and buoyancy forcing makes the isothermal layer in the western part of the western Pacific warm pool quite different from that in the eastern part of the western Pacific warm pool. Figure 8d shows that the winds from the central to eastern Pacific are strong and stable. In contrast, the winds in the western side are weak on average, and highly intermittent. The strong (weak) winds at the central (western) side correspond to the low (high) stratification area (Fig. 8a). For radiation flux, distribution of solar radiation in the western side is lower than the eastern side of the equatorial Pacific. However, the distribution of the mean solar radiation in the west side is still higher than 200 W/m² (Fig. 9 of Wirasatriya et al. 2015). The relationship between buoyancy forcing and thermal stratification in the western equatorial Pacific has been investigated by Lukas and Lindstorm (1991). The strong and stable stratification at the western side is caused by the strong buoyancy forcing associated with an excess of precipitation over evaporation. Thus, the more stratified and warmer layer in the western

Fig. 12 Schematic diagram of the vertical thermal structure of HE. Lower to higher temperature is represented by yellow, orange, and red colors
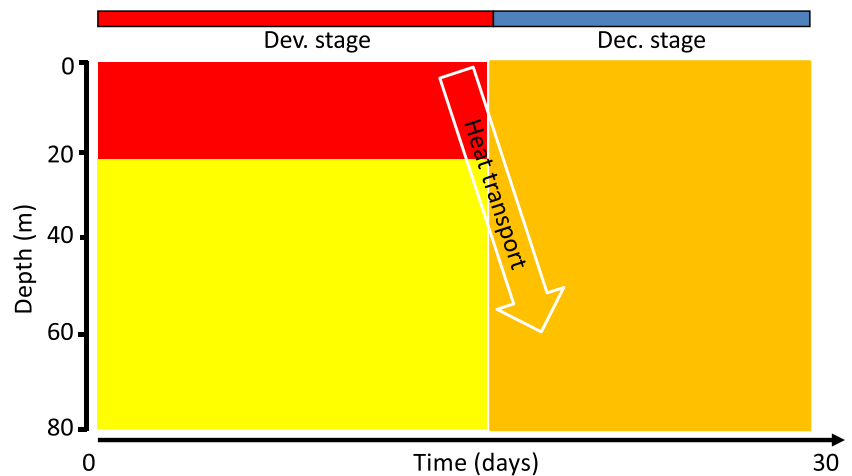
Pacific warm pool is formed by high solar radiation more than 200 W/m², and higher precipitation and lower wind speed than the eastern side of the equatorial Pacific. At the eastern side, the evaporation rate is larger than precipitation rate. However, the influence of stable and strong wind speed is dominant over the influence of evaporation excess. As a result, strong and stable easterly wind can induce the equatorial upwelling.

Through the concept of the vertical thermal structure of HEs, we emphasize that the process of radiative heating at the surface does not occur simultaneously with the heat transport controlled by the wind forcing and this may characterize the heat transport mechanisms in the isothermal layer of the Pacific warm pool. This step-by-step process may be more efficient in distributing the heat received at the sea surface and transmitted to the deeper layer. As shown in Fig. 9, although both radiative forcing and wind forcing were strong in 2010, less heat was transported to the deeper layer. Therefore, the vertical thermal structure of the HE can become a new perspective of heat input mechanisms into the isothermal layer in the western equatorial Pacific.

We realize that the ocean dynamics that controls the variability of western Pacific warm pool is very complex. The influences of equatorial wave such as Kelvin and Rossby waves that generate downwelling and upwelling actions, then subduction, entrainment, and also lateral mixing, which regulate oceanic heat budget in the warm pool, were neglected in the present study. For a long periodic event like El Niño Southern Oscillation, Hu et al. (2017) found that the low SST band in the western Pacific warm pool along 10°N during El Niño is caused by the upwelling generated by the westward propagating Rossby wave. This low SST band is known as the split of western Pacific warm pool. Furthermore, the zonal heat advection in the eastern edge of the split region also contributes to the split process of the western Pacific warm pool. Meanwhile, equatorial Kelvin waves may also lead to short-term cooling and warming that control the mixed layer temperature in the equatorial Pacific region as has been presented by Rydbeck et al. (2019). On the other hand, the present study only focus on the vertical heat transport during the decay stage of HE that contribute to the sustainment of the warmness of the isothermal layer in the western Pacific warm pool.

Therefore, further investigations involving all possible factors and more HE cases may lead to a better understanding of the HE contribution to the formation of warm isothermal layer in the Pacific warm pool. This becomes the promising topics for the future study.

For buoyancy forcing, Wirasatriya et al. (2017) indicated that the increasing SST during the development stage of HE was related to the existence of barrier layer formed by the high precipitation that occurred before the development stage. For the case of HE030528, the occurrence of high precipitation prior to the development stage causes the formation of barrier layer denoted by the thin low density layer from the surface layer to about 20 m depth during the development stage (Fig. 10). This barrier layer may keep the solar heating only in the surface layer leading to the increasing SSTs during the development stage. During the decay stage, the density increases as the convergence brings fresher water in the surface to the deeper layer. The high precipitation prior to the development stage of HE030528 is related to the active phase of Madden Julian Oscillation. However, out of 71 HE cases, Wirasatriya et al. (2017) found only 29 HE cases that are related to the MJO. Thus, this mechanism is not dominant for HE generation.

Qin et al. (2008) compared the thermal structure between HE0611-east and HE0611-west in the western equatorial Pacific. Although the thermal stratification was detected during the occurrence of HE0611-west, the vertical thermal structure of HE was not apparent in their analysis. This is because their analysis only focused on the development stage. As shown in Fig. 4 of Qin et al. (2008), the integrated heat input of HE0611-west still increased toward the end point of their analysis. As stated in the previous section, the decay stage is important to show the accumulated heat distributions, i.e., how the accumulated heat is released to the atmosphere and transported to the subsurface layer. Therefore, the typical vertical thermal structure of the HE0611-west as explained in the previous section can only be obtained by observing both stages of HE.

Wirasatriya et al. (2016) demonstrated the atmospheric structure associated with HE030528 in the western equatorial Pacific. Combining their findings with the oceanic structure revealed in

the present study, a whole picture of a HE is depicted schematically in Fig. 11. During the development stage, surface wind speed and surface wind convergence are low. In the atmosphere, the weak surface wind influences the convection process by reducing the latent heat flux as well as the evaporation rate. Because of the decreasing convection, dry air from the top of troposphere sank and gave positive feedback to suppress the convection. The subsidence area corresponds to the clear sky area which leads to the high solar radiation during the development stage of the HE030528. In the ocean, the weak surface winds prevent oceanic mixing. Thus, during the development stage, the increase of SSTs of more than ~ 30 °C is caused by the accumulated heat received by the sea surface from the solar radiation (Fig. 11-left). During the decay stage, surface wind speed and convergence are high. The strong convergence activates the convection process and accelerates the cloud formation. Eventually, the solar radiation decreases. The strong wind speed increases the latent heat release to the atmosphere and induces the downwelling that transports the heat to the deeper layer of the isothermal layer. These processes reduce SSTs in the decay stage (Fig. 11-right).

5 Conclusions

In this section, we summarize the mechanisms of HE formation observed from the perspective of oceanic structure and the role of HEs for the formation of the western Pacific warm pool.

1. Oceanic structure during HE occurrences involves the heat accumulation which is received by the sea surface during the development stage and the heat release to the atmosphere and the heat transport to deeper layers during the decay stage.

2. We derived typical vertical thermal structure and its temporal variation during HEs. Temperature is higher in the surface layer (0–20 m) than in deeper layers (20 m – thermocline layer), creating strong thermal stratification in the surface layer during the development stage. During the decay stage, temperature in the surface layer (deeper layer) decreases (increases), which causes temperature in the water column become more uniform. The vertical thermal structure of HE is shown systematically in Fig. 12.

3. During the development stage, low wind speed stabilizes the water column and together with the high solar radiation, heat gain is accumulated only in the sea surface, increasing the temperature in the surface layer. During the decay stage, solar radiation is low and the occurrence of strong westerly wind activates the current convergence process that transports accumulated heat from the surface to the deeper layer which causes the temperature in the water column to become more uniform. This mechanism explains the formation of the vertical thermal structure of HE.

4. The vertical thermal structure of HE also can be an indication of the role of HE in maintaining the warm isothermal layer in the western Pacific warm pool. The more HE occurrence, the more heat is transported to the deeper layer and this can keep the warm isothermal layer in the western Pacific warm pool. In contrast, the absence of HE leads to the absence of the heat transported to the deeper layer which results in decreasing temperature in the isothermal layer in the western Pacific warm pool. Thus, although HE is categorized as the short-term (< 1 month) and high SST (> 30 °C) phenomenon, its frequent occurrence can affect the long-term SST pattern as represented by the formation of the western Pacific warm pool.

References

Akima H (1996) Algorithm 761 - scattered-data surface fitting that has the accuracy of a cubic polynomial. Assoc Comput Machin Transact Math Softw 22(3):362–371

Anderson SP, Weller RA, Lukas RB (1996) Surface buoyancy forcing and the mixed layer of the western Pacific warm pool: observation and 1d model result. J Clim 9:3056–3085

Ando K, McPhaden MJ (1997) Variability of surface layer hydrography in the tropical Pacific Ocean. J Geophys Res 102(C10):23063–23078

Bathen KH (1972) On the seasonal changes in the depth of the mixed layer in the North Pacific Ocean. J Geophys Res 77:7138–7150

Clement A, Seager R (1999) Climate and the Tropical Ocean. J Clim 12:3383–3400

Clement A, Seager R, Murtugudde R (2005) Why are there tropical warm pools? J Clim 18:5294–5310

Garric G, Parent L (2018a) Product user manual for Global Ocean reanalysis products GLOBAL-REANALYSIS-PHY-001-025. Version 4.1. Marine Copernicus eu. http://resources.marine.copernicus.eu/documents/PUM/CMEMS-GLO-PUM-001-025.pdf. Accessed on 2 September 2019

Garric G, Parent L (2018b) Quality information document for Global Ocean reanalysis products GLOBAL-REANALYSISPHY-001-

025. Marine Copernicus eu. http://resources.marine.copernicus.eu/documents/QUID/CMEMS-GLO-QUID-001-025.pdf Accessed on 2 September 2019

Herweijer C, Seager R, Winton M, Clement A (2005) Why ocean heat transport warms the global mean climate. Tellus 57a:662–675

Hosoda K (2013) Empirical method of diurnal correction for estimating sea surface temperature at dawn and noon. J Oceanogr 69:631–646. https://doi.org/10.1007/s10872-013-0194-4

Hosoda K, Kawamura H, Sakaida F (2015) Improvement of new Generation Sea surface temperature for Open Ocean (NGSST-O): a new sub-sampling method of blending microwave observations. J Oceanogr 71:205–220. https://doi.org/10.1007/s10872-015-0272

Hu S, Hu D, Guan C, Xing N, Li J, Feng J (2017) Variability of the western Pacific warm pool structure associated with El Niño. Clim Dyn 49(7–8):2431–2449. https://doi.org/10.1007/s00382-016-3459-y

Huffman G, Bolvin D, Braithwaite D, Hsu K, Joyce R, Xie P (2014) Integrated multi-satellitE retrievals for GPM (IMERG), version 4.4. NASA's precipitation processing center, accessed 31 January, 2015, ftp://arthurhou.pps.eosdis.nasa.gov/gpmdata/

Kawamura H, Qin H, Ando K (2008) In-situ diurnal sea surface temperature variations and near-surface thermal structure in the tropical hot event of the indo-Pacific warm pool. J Oceanogr 64:847–857

Lukas R (1988) On the role of western Pacific air-sea interaction in the El Nino/southern oscillation phenomenon. Proceedings of the U.S. TOGA-8, University Corporation for Atmospheric Research, Boulder, Colorado

Lukas R, Lindstorm E (1991) The mixed layer of the western equatorial Pacific Ocean. J Geophys Res 96(S01):3343–3357. https://doi.org/10.1029/90JC01951

Marshall J, Plumb RA (2008) Atmosphere, Ocean and Climate Dynamics: An Introductory Text. Elsevier Academic Press, Cambridge

McPhaden MJ, Ando K, Bourles B, Freitag HP, Lumpkin R, Masumoto Y, Murty VSN, Nobre P, Ravichandran M, Vialard J, Vousden D, Yu W (2009) The global tropical moored buoy array. In hall J, Harrison DE, stammer D (eds) proceedings of the "OceanObs '09: Sustained Ocean observations and information for society" conference, vol 2, 723 Venice, Italy, ESA publication, WPP-306. https://doi.org/10.5270/OceanObs09.cwp.61

Qin H, Kawamura H (2009a) Atmosphere response to a hot SST event in November 2006 as observed by AIRS instrument. Adv Space Res 44:395–400. https://doi.org/10.1016/j.asr.2009.03.003

Qin H, Kawamura H (2009b) Surface heat fluxes during hot events. J Oceanogr 65:605–613

Qin H, Kawamura H (2010) Air-sea interaction throughout the troposphere over a very high sea surface temperature. Geophys Res Lett 37:1–4. https://doi.org/10.1029/2009GL041685

Qin H, Kawamura H, Kawai Y (2007) Detection of hot event in the equatorial indo-Pacific warm pool using advanced satellite sea surface temperature, solar radiation, and wind speed. J Geophys Res 112:C07015. https://doi.org/10.1029/2006JC003969

Qin H, Kawamura H, Sakaida F, Ando K (2008) A case study of the tropical hot event in November 2006 (HE0611) using a geostationary meteorological satellite and the TAO/TRITON mooring array. J Geophys Res 113:C08045. https://doi.org/10.1029/2007JC004640

Renka RJ, Cline AK (1984) A Triangle-based C1 Interpolation Method. Rocky Mountain Journal of Mathematics 14(1): 223-237

Rydbeck AV, Jensen TG, Flatau M (2019) Characterization of Intraseasonal kelvin waves in the equatorial Pacific Ocean. J Geophys Res 124(3):2028–2053. https://doi.org/10.1029/2018JC014838

Waliser DE (1996) Formation and limiting mechanisms for very high sea surface temperature : Linking the dynamics and the thermodynamics. J Climate 9:161–188

Waliser DE, Graham NE (1993) Convective cloud systems and warm-pool sea-surface temperatures: coupled interactions and self-regulation. J Geophys Res 98(D7):12881–12893

Wirasatriya A, Kawamura H, Shimada T, Hosoda K (2015) Climatology of hot events in the western equatorial Pacific. J Oceanogr 71:77–90. https://doi.org/10.1007/s10872-014-0263-3

Wirasatriya A, Kawamura H, Shimada T, Hosoda K (2016) Atmospheric structure favoring high sea surface temperatures in the western equatorial Pacific. J Geophys Res 121:1–14. https://doi.org/10.1002/2016JD025268

Wirasatriya A, Sugianto DN, Helmi M (2017) The influence of madden Julian oscillation on the formation of the hot event in the Western equatorial Pacific, 2nd international conference on tropical and coastal region eco development 2016, IOP Conf. Series: Earth Environ Sci 55:012006. https://doi.org/10.1088/1755-1315/55/1/012006

Wirasatriya A, Sugianto DN, Helmi M, Maslukah L, Widiyandono RT, Herawati VE, Subardjo P, Handoyo G, Haryadi MJ, Suryoputro AAD, Atmodjo W, Setiyono H (2019) Heat flux aspects on the seasonal variability of sea surface temperature in the Java Sea. Ecol Environ Conserv 25(1):434–442

Wyrtki K (1964) The thermal structure of the eastern Pacific Ocean. Dstch Hydrography Zeitzschel, Ergänzungsheft A 8:6–84

Wyrtki K (1989) *Some thoughts about the west Pacific warm pool*. Paper presented at Western Pacific international meeting and workshop on TOGA COARE, Nouméa, New Caledonia 99-109

Yu L, Weller RA (2007) Objectively Analyzed air-sea heat Fluxes for the global ice-free oceans (1981–2005). Bull Am Meteor Soc 88: 527–539